



Cite this: *Phys. Chem. Chem. Phys.*,
2019, 21, 26017

Single photon ionization of methyl isocyanide and the subsequent unimolecular decomposition of its cation: experiment and theory†

A. Bellili,^a Z. Gouid,^{ab} M. C. Gazeau,^b Y. Bénilan,^b N. Fray,^b J. C. Guillemin,^{ib}^c
M. Hochlaf^{ib}*^a and M. Schwell^{ib}*^b

Methyl isocyanide, CH₃NC, is a key compound in astrochemistry and astrobiology. A combined theoretical and experimental investigation of the single photon ionization of gas phase methyl isocyanide and its fragmentation pathways is presented. Vacuum ultraviolet (VUV) synchrotron radiation based experiments are used to measure the threshold photoelectron photoion coincidence (TPEPICO) spectra between 10.6 and 15.5 eV. This allowed us to experimentally determine the adiabatic ionization energy (AIE) and fragment ion appearance energies (AE) of gas-phase methyl isocyanide. Its AIE has been measured with a precision never achieved before. It is found to be AIE_{exp} = 11.263 ± 0.005 eV. We observe a vibrational progression upon ionization corresponding to the population of vibrational levels of the ground state of the methyl isocyanide cation. In addition, four fragment ion appearance energies (AEs) were measured to be AE (*m/z* 40) = 12.80 ± 0.05 eV, AE (*m/z* 39) = 13.70 ± 0.05 eV, AE (*m/z* 15) = 13.90 ± 0.05 eV, AE (*m/z* 14) 13.85 ± 0.05 eV, respectively. In order to interpret the experimental data, we performed state-of-the-art computations using the explicitly correlated coupled cluster approach. We also considered the zero-point vibrational energy (ZPVE), core-valence (CV) and scalar relativistic (SR) effects. The results of theoretical calculations of the AIE and AEs are in excellent agreement with the experimental findings allowing for assignment of the fragmentations to the loss of neutral H, H₂, CN and HCN upon ionization of CH₃NC. The computations show that in addition to the obvious bond breakings, some of the corresponding ionic fragments result from rearrangements – upon photon absorption – either before or after electron ejection.

Received 2nd August 2019,
Accepted 26th September 2019

DOI: 10.1039/c9cp04310a

rsc.li/pccp

1. Introduction

Among the molecules observed in the interstellar medium (ISM), organic and inorganic cyanides (or nitriles) are an important class of compounds. They represent approximately 20% of the more than 200 molecules observed today in the ISM gas phase.¹ Cyanides (R–C≡N) are easily detectable in a number of interstellar environments because of their large abundances.^{2–5} Very recently, even fairly complex cyanides like hydroxyacetonitrile⁶ and benzonitrile⁷ have been detected. Since the observation of R–C≡N molecules, a few isomers with the functional group

–N≡C, called isocyanides (or isonitriles; R–N≡C), have also been detected in objects of the ISM. They include HNC,^{3,8} CH₃–NC^{5,9–14} HC≡C–NC,¹⁵ CH₂CH–NC⁵ (tentatively) as well as inorganic isocyanides.¹ CH₃CH₂–NC has also been searched for and upper limits of the column densities were derived recently.¹³ Basic photophysical data are often unknown for these compounds.

Methyl isocyanide, CH₃–N≡C, the object of this vacuum ultraviolet (VUV) spectroscopic study and denoted “MIC” in the following, is a thermodynamically less stable isomer of CH₃–C≡N, the latter being one of the most common molecules in the ISM. MIC was claimed to be detected for the first time in 1984 towards the cold cloud TMC1⁹ but the first secure detection towards the high-mass star-forming region Sgr B2 was reported in 1988.¹⁰ The presence of MIC in the cold clouds of Sgr B2(N) was confirmed seventeen years later by Remijan *et al.*¹¹ MIC has also been detected in the Horsehead nebula photodissociation region (PDR)¹² and in Orion-KL.⁵ Very recently, Margulès *et al.* confirmed the detection of MIC in Sgr B2 and Orion-KL.¹³ These authors analyzed in depth all available MIC observations using isomeric abundance ratios $r = [\text{R–N}\equiv\text{C}]/[\text{R–C}\equiv\text{N}]$ as a tool to

^a Université Paris-Est, Laboratoire Modélisation et Simulation Multi Echelle, MSME UMR 8208 CNRS, 5 bd Descartes, 77454 Marne-la-Vallée, France. E-mail: hochlaf@univ-mv.fr

^b Laboratoire Interuniversitaire des Systèmes Atmosphériques, LISA, UMR CNRS 7583, Université Paris-Est-Créteil, Université de Paris, Institut Pierre Simon Laplace, 94010 Créteil, France. E-mail: martin.schwell@lisa.u-pec.fr

^c Univ Rennes, Ecole Nationale Supérieure de Chimie de Rennes, CNRS, ISCR UMR6226, F-35000 Rennes, France

† Electronic supplementary information (ESI) available. See DOI: 10.1039/c9cp04310a

constrain chemical routes for formation and destruction in order to explain the presence of R-NC (R = methyl, vinyl, ethyl) in a large range of interstellar environments. For example, the observation of MIC (with $r = 0.01$) in warm regions of Sgr B2 points to a possible grain chemistry pathway for its production because isomerization from CH_3CN to CH_3NC is very unfavorable under thermal conditions. In this context, dedicated laboratory experiments have shown that desorption of MIC from interstellar grains is slightly facilitated compared to the isomer CH_3CN because MIC is less tightly bound to the studied grain analogues.^{16,17} This would lead to a gas phase enrichment of CH_3NC at a given grain temperature compared to the abundance ratio in the condensed phase. On the other hand, Remijan *et al.*,¹¹ have concluded, from their Sgr B2(N) observations, that large-scale, non-thermal processes such as shocks or enhanced UV flux may account for the conversion of CH_3CN to CH_3NC . This conclusion is confirmed by the observation of MIC in the Horsehead nebula PDR, with a fairly large relative abundance of $r = 0.15$.¹² Laboratory experiments performed by Hudson and Moore,¹⁸ on a number of different organic cyanides, have shown that these can undergo, with significant yields, isomerization to isocyanides upon irradiation with 0.8 MeV protons and also with VUV radiation. We also mention that the interconversion $\text{CH}_3\text{CN} \rightleftharpoons \text{CH}_3\text{NC}$ has been studied by high-level theoretical calculations very recently.¹⁹

In this astrophysical context, the knowledge of basic photo-physical data, including ionization and fragmentation energies, is crucial to go further in the interpretation of interstellar abundances and to model the chemistry occurring in these media. The study of the photoionization and dissociative photoionization of MIC is particularly relevant since the edges of molecular clouds, for example, are subject to intense VUV irradiation. In the past, our group has investigated the VUV photophysics of several cyanides that are key compounds in astrochemistry and astrobiology. We have studied methyl cyanide (CH_3CN ^{20,21}), cyanoacetylenes (HC_3N ²² and HC_5N ²³), acetyl cyanide ($\text{CH}_3\text{C(O)CN}$ ²⁴), and aminoacetonitrile ($\text{H}_2\text{NCH}_2\text{CN}$ ²⁵). To date, isonitriles were rarely studied by VUV spectroscopy, therefore laboratory photophysical data are scarce. This is the case of MIC since to the best of our knowledge, only HeI and HeII photoelectron spectra^{26–28} and a VUV absorption spectrum in arbitrary intensity units in the energy range 7.3–11.8 eV²⁹ have been reported in literature.

Here we want to step forward towards the understanding of methyl isocyanide photochemistry. The main aim of this work is to give insight into the stability and reactivity of MIC under interstellar radiation fields. Since the early studies mentioned above, the VUV spectroscopy of MIC has not been reinvestigated. In this work, we use threshold photoelectron photoion coincidence (TPEPICO) spectroscopy³⁰ in connection with VUV synchrotron radiation from the DESIRS beamline of the French synchrotron SOLEIL. The adiabatic ionization energy (AIE) has been measured with high precision as well as fragment ion appearance energies up to a photon energy of 15.5 eV. Several fragment ions are observed in this energy domain. The assignment and the interpretation of all experimental data require

high-level *ab initio* calculations. The ionization and the appearance energies of cationic fragments have been computed using explicitly correlated coupled cluster calculations, considering different dissociative ionization pathways. We also took into account the zero-point vibrational energy, core-valence and scalar relativistic effects. In order to interpret the observed vibronic structure, harmonic and anharmonic frequencies of the ground state of the cation have been calculated.

2. Methods

2.1. Experimental methods

The experiments were carried out at the DESIRS beamline of the French synchrotron facility SOLEIL in connection with its 6.65 m normal incidence monochromator and the photoelectron photoion coincidence (PEPICO) spectrometer DELICIOUS III.³¹ This spectrometer allows for full momentum detection of the ions and velocity map imaging (VMI) of the electrons at the same time, but in exactly opposite directions. Ions and electrons are detected in coincidence and their collection is perpendicular to (i) the molecular beam inlet and (ii) the VUV light propagation direction (all 90° setup). More details on this set-up and the experimental operating conditions can be found elsewhere.³¹ For our measurements, we used the 200 g mm⁻¹ grating of the monochromator with entrance/exit slit widths of typically 100 μm/100 μm yielding a spectral resolution (photons) of 0.72 Å (about 6 meV at 10 eV). (T)PEPICO spectra are normalized by the photon flux measured by a photodiode (AXUV, IRD) placed after the photoionization region. For better spectral purity of the beamline, we use a gas filter that is filled with 0.25 mbar of Ar. This allows for effective suppression of either higher energy stray light of the electron storage ring or higher order radiation from the undulator. The presence of Ar absorption lines in the spectrum arising from this filter furthermore allows for calibration of the energy scale to an absolute accuracy of about 1 meV.

2.2. Preparation of methyl isocyanide

CH_3NC has been synthesized following Schuster *et al.*³² with some modification. *N*-Methylformamide (5.9 g, 100 mmol), *p*-toluenesulfonyl chloride (38.1 g, 200 mmol), and trioctylamine (70.7 g, 200 mmol) were introduced into a one-necked round-bottomed flask equipped with a stirring bar. The flask was fitted on a vacuum line (0.1 mbar) equipped with two U-tubes with stopcocks. The first one was immersed in a liquid nitrogen cold bath. The apparatus was evacuated, the pressure was then stabilized at 2 mbar and the mixture allowed to warm to 80 °C over about 1 h. MIC was thus evacuated from the reaction mixture as it was formed and condensed in the trap. At the end of the reaction, the trap was allowed to warm to room temperature, and the pure compound was condensed in the second trap cooled to -100 °C. Yield: 3.3 g, 80%. MIC, a colorless, bad-smelling liquid, is kept under nitrogen in the freezer for storage.

For the measurements, a quartz glass recipient with a few mL of MIC is allowed to warm up to room temperature. The evacuated

recipient is directly connected to the molecular beam inlet *via* an adjustable needle valve. The saturation vapor pressure of MIC is such that no additional heating is necessary for the measurements. Helium is used as a carrier gas in the molecular beam inlet.

2.3. Theoretical methods

The main aim of the present computations is to provide an interpretation of the experimental spectra. For that purpose, we map the potential energy surfaces (PESs) of MIC and of its cation, MIC⁺. These PESs cover the equilibrium structures and the lowest cationic fragmentation channel regions. All electronic computations are carried out using GAUSSIAN09³³ and MOLPRO (version 2015) package³⁴ in the C₁ point group.

We start our computations by geometry optimizations (opt) of MIC and MIC⁺ molecular structures, as well as the fragments of MIC⁺ at the PBE0/aug-cc-pVDZ level^{35–37} of theory (using the ultrafine integral grids). These computations are followed by harmonic frequencies calculations to attest the nature of the stationary points found (either a minimum or a transition state). The anharmonic frequencies are obtained from the derivatives (second, third, and fourth) of the potentials and second-order perturbation theory treatment of nuclear motions as implemented in GAUSSIAN 09. Note that this procedure did not allow to account for possible anharmonic resonances or large amplitude motion vibrational modes. The latter need full variational treatments, which are out of the scope of this work.

Afterwards, we perform single point (SP) computations at the (R)CCSD(T)-F12(b)/cc-pVTZ-F12 (+CV+SR+ZPVE) level to derive more accurate energetics. Briefly, single-point calculations, based on the optimized structures, are done using the (R)CCSD(T)-F12 (approximation b) explicitly correlated method^{38–40} in conjunction with the cc-pVTZ-F12 explicitly correlated basis sets⁴¹ and the corresponding auxiliary basis sets and density-fitting functions.^{42–45} Then, we include the core-valence (CV, as the difference between CCSD(T)/cc-pwCVTZ^{46,47} energies with and without considering 1s electrons) and scalar-relativistic (SR, as the difference between CCSD(T)/cc-pVTZ-DK^{48–50} and CCSD(T)/cc-pVTZ energies) corrections. The zero-point vibrational energy correction (ZPVE) is obtained at the PBE0/aug-cc-pVDZ level. Through benchmarks and comparisons to experiment, we showed earlier that the PBE0/aug-cc-pVDZ(opt)/(R)CCSD(T)-F12/cc-pVTZ-F12 (+CV+SR+ZPVE) (SP) composite scheme allows for prediction of ionization energies and appearance energies (to within ±0.005 eV) with reduced cost.^{51–57}

We also computed the photoelectron spectrum of MIC following the method implemented in GAUSSIAN 09, which consists on a Franck Condon (FC) analysis followed by a simulation of the vibrationally resolved electronic spectrum by means of the Time-Independent Adiabatic Hessian Franck-Condon (TI-AH|FC) model.^{58–61}

3. Results and discussion

We present a combined theoretical and experimental investigation on the single photon ionization of the methyl isocyanide molecule in the gas-phase, in the 10.5 to 15.5 eV energy range

and the subsequent unimolecular decomposition processes. Calculations were carried out in order to assign the observed ionization and fragmentation thresholds. To this end, a calibrated method of theory was applied. Further calculations were performed with the aim to elucidate the structure of fragment ions experimentally observed as well as the observed vibrational progression.

3.1. Photoionization mass spectra

Fig. 1a shows the photoionization mass spectra of MIC collected after single photon ionization at different photon energies in the range from 12 to 15.5 eV (12, 13.5, 14, 14.5, 15 and 15.5 eV). All the spectra have been normalized to the base peak, at *m/z* 41 corresponding to the parent ion CH₃NC⁺. The mass region of the parent ion is shown in Fig. 1a, between *m/z* 37 and *m/z* 43. We can identify four peaks with different intensities: the most intense peak, at *m/z* 41, corresponds to the parent ion CH₃NC⁺. At increasing photon energy two peaks at *m/z* 40 and *m/z* 39 with lower intensity appear, corresponding respectively to the loss of atomic hydrogen and molecular hydrogen (or potentially 2H). They are assigned to fragments with elemental formulas C₂H₂N⁺

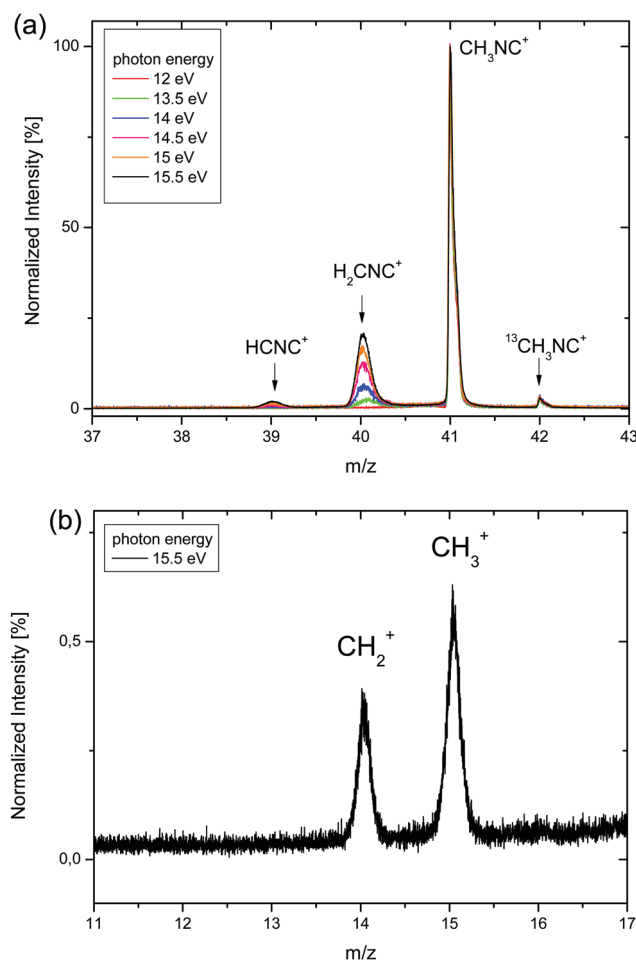


Fig. 1 Time-of-flight mass spectra of methyl isocyanide recorded between 12 and 15.5 eV photon energies (0.5 eV step width). (a) Region of the parent cation *m/z* 41. (b) Region below *m/z* 17.

and C_2HN^+ . The ^{13}C isotopomer of the parent ion CH_3NC^+ is also visible at m/z 42 with the expected natural isotopic abundance ratio. In Fig. 1b, we show a mass spectrum recorded at 15.5 eV from m/z 11 to m/z 17. In this zoom two fragment ions at m/z 15 and m/z 14 are seen but with very weak intensity. These mass peaks are assigned to the fragments CH_3^+ and CH_2^+ respectively formed by the loss of CN and HCN (or HNC) molecules.

3.2. Ionization and fragmentation thresholds

Fig. 2 presents the threshold photoelectron photoion coincidence (TPEPICO) spectrum of m/z 41. One can see the vibronic progression of the ground electronic state of CH_3NC^+ . This band structure has been observed in the earlier HeI photoelectron spectra, but with much less spectral resolution.^{26,27} The first band corresponds to the MIC $0_0^0 \rightarrow MIC^+$ photoionization transition. The other bands are due to the population of the lowest vibrational levels of the cation upon ionizing the neutral MIC. Their tentative assignment shown also in Fig. 2 is discussed in Section 3.3.

The experimental adiabatic ionization energy (AIE) of MIC can be measured from the TPEPICO spectrum being the center of the first and most intense band (indicated by a vertical dotted line in Fig. 2). This band is assigned to the 0_0^0 origin of the progression and corresponds to the transition from the neutral ground state to the ground state of the cation. We can deduce $AIE_{exp} = 11.263 \pm 0.005$ eV. This value has never been measured with such a precision. In the earlier HeI photoelectron spectra, values with a large spread of 11.24 eV,²⁶ 11.27 eV,²⁷ and 11.32 eV,²⁸ are reported by three different groups (no error bars are given in the earlier studies). Also, our experimental finding is in excellent agreement with the theoretical AIE value being $AIE_{calc} = 11.265$ eV. In this study AIE_{calc} has been calculated at the PBE0/aug-cc-pVDZ(opt)//(R)CCSD(T)-F12/cc-pVTZ-F12 (+CV+SR+ZPVE) (SP) level (for more details see Table S1 of the ESI†). It falls into the precision interval of the experimental AIE given above.

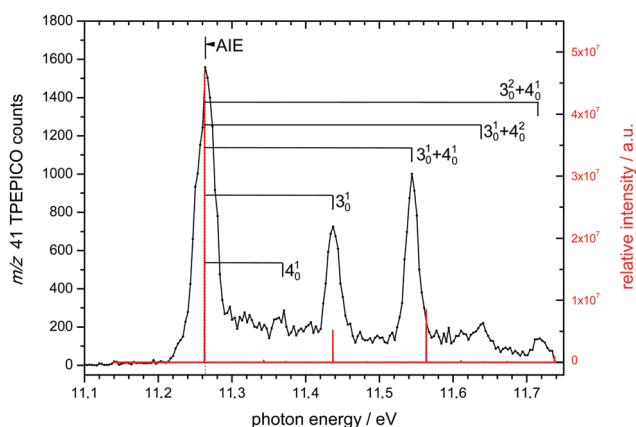


Fig. 2 TPEPICO spectrum of the methyl isocyanide parent ion (m/z 41). The experimental adiabatic ionization energy (AIE) is taken as the median of the 0_0^0 band (indicated by a bar and a vertical dotted line). The assignment of the vibrational progression is discussed in the text. Red sticks correspond to the computed photoelectron spectrum of MIC (Franck Condon analysis followed by a simulation of the vibrationally resolved electronic spectrum).

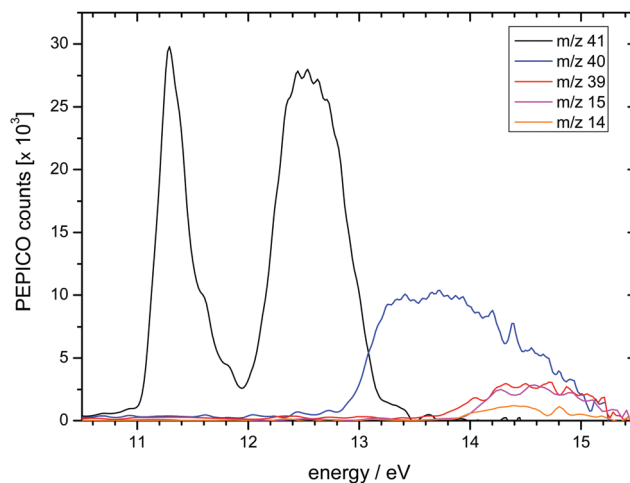


Fig. 3 PEPICO spectra of the CH_3NC^+ parent ion and 4 fragment ions observed in the 10.5 to 15.5 eV energy range. These spectra are recorded with a fixed energy VMI image taken at a photon energy of $h\nu = 15.5$ eV. The energy scale is constructed as the difference of the kinetic energy scale of the position sensitive electron detector and $h\nu = 15.5$ eV (for details see ref. 31).

This is in line with recent precise determinations of AIEs of medium-sized molecular systems using similar experimental and theoretical approaches.^{52–57}

Fig. 3 shows the PEPICO spectra of the five cations observed in Fig. 1 (m/z 41, 40, 39, 15, 14), in the 10.6–15.5 eV energy range. These PEPICO spectra are derived from a fixed photon energy VMI image (at $h\nu = 15.5$ eV) taken at a repeller voltage permitting the detection of all photoelectrons on the circular detector, as a function of their kinetic energy KE_{el} and in coincidence with the cation of the respective m/z ratio. The energy scale in Fig. 3 is constructed as the difference of the kinetic energy scale of the position sensitive electron detector and $h\nu = 15.5$ eV (for details see ref. 31). In this type of PEPICO spectra the spectral resolution is low (the step-width is 18 meV) but sufficient for AE determinations with 0.05 eV precision. The m/z 41 PEPICO spectrum shows two bands peaking at 11.29 and 12.53 eV corresponding respectively to the ionization of n_C and π_{NC} electrons according to Bevan *et al.*²⁷ We note that, below 12.8 eV, the parent ion m/z 41 PEPICO spectrum represents a relative photoionization efficiency curve being proportional to the total photoionization cross section of MIC in this energy region. Dissociative photoionization processes take place only above 12.8 eV. Relative partial and total ionization cross sections can be determined from these data. The experimental appearance energies (AEs) are set to the energy position where the ion signal exceeds the background level and starts rising (see Fig. F1a–d provided in the ESI†).

Table 1 summarizes the measured AEs together with the results from the quantum-chemical calculations (*cf.* Table S2 in the ESI† for more details). The appearance energy of the intense fragment ion m/z 40 has been measured to be $AE_{exp}(C_2H_2N^+) = 12.80 \pm 0.05$ eV. This mass is due to an ion formed by H loss reaction corresponding to the $CH_3NC + h\nu \rightarrow C_2H_2N^+ + H + e^-$ reaction. The question as to which $C_2H_2N^+$ isomer is formed is

Table 1 Calculated and measured appearance energies (AEs) of the different fragmentation pathways of the resulting cation of methyl isocyanide. These AEs (in eV) are computed at the PBE0/aug-cc-pVDZ(opt)//(R)CCSD(T)-F12/cc-pVTZ-F12 (+CV+SR+ZPVE) (SP) level. For more details, see Table S2 of the ESI

| <i>m/z</i> | 40 | | 39 | | 15 | 14 |
|-----------------------|--|-------------------------------------|------------------------------------|--|---|------------------------------------|
| Fragmentation channel | H + H ₂ CNC ⁺ | H + H ₂ CCN ⁺ | H ₂ + HCCN ⁺ | H ₂ + HCNC ⁺ | CN + CH ₃ ⁺ | HCN + CH ₂ ⁺ |
| Cal. ^a | 13.499 | 12.881 | 13.940 | 13.708 | 14.05 | 13.812 |
| Exp. | 12.80 ± 0.05 ^a 13.21 ± 0.04 ^b 13.21 ^c | | | 13.70 ± 0.05 ^a 14.56 ± 0.08 ^b 14.46 ^c | 13.90 ± 0.05 ^a 14.76 ^c | 13.85 ± 0.05 ^a |

^a This work. ^b Electron impact ionization, ref. 62. ^c Electron impact ionization, ref. 63.

discussed below. The second observed fragmentation is associated with the reaction channel $\text{CH}_3\text{NC} + h\nu \rightarrow \text{C}_2\text{HN}^+ + \text{H}_2 + \text{e}^-$. Elimination of two separate hydrogen atoms can be discarded since this channel would be much higher in energy given the H₂ dissociation energy of 4.52 eV. We measure $\text{AE}_{\text{exp}}(\text{C}_2\text{HN}^+) = 13.70 \pm 0.05$ eV. Also in this reaction, at least two isomers of the fragment C_2HN^+ can be expected either HCCN^+ or HCNC^+ . The AE of the *m/z* 15 ion, visible upon zooming in the baseline in Fig. 1b, is determined experimentally to be $\text{AE}_{\text{exp}} = (13.90 \pm 0.05)$ eV. This ion is produced *a priori* by loss of CN giving rise to the reaction $\text{CH}_3\text{NC} + h\nu \rightarrow \text{CH}_3^+ + \text{CN} + \text{e}^-$. The AE of *m/z* 14, with similar, low intensity in the TOF-MS shown in Fig. 1b, is determined experimentally to be $\text{AE}_{\text{exp}} = 13.85 \pm 0.05$ eV. This fragmentation pathway corresponds to the loss of a species of the elemental formula HCN giving rise to the dissociative reaction $\text{CH}_3\text{NC} + h\nu \rightarrow \text{e}^- + \text{CH}_2^+ + \text{HCN}$ (or HNC). Table 1 shows that our AEs are much lower than those measured earlier using electron impact (EI) ionization by Harland and McIntosh⁶² and by Heerma and deRidder.⁶³ We have discussed recently⁵³ that AEs measured by EI ionization are generally too high, mainly because with EI fewer ions are formed in the ion source and by consequence the instrument's sensitivity is lower. Since reaction rates increase smoothly in the threshold region, this yields too high AEs.

Furthermore, ion transmission efficiencies of quadrupole mass analyzers used in the past are poor and thus the sensitivity of these instruments is further lowered in comparison with modern Time-of-Flight instruments. Both effects lead to too high AE values which can be off by 1 eV easily.

In order to understand in more detail these fragmentation processes and in particular the chemical structure of the cationic and neutral fragments formed by the dissociative photoionization processes, we have undertaken quantum-chemical calculations of the different fragmentation pathways presented in Fig. 4. The results are summarized in Table 1. For the *m/z* 40 ($\text{C}_2\text{H}_2\text{N}^+$) formed by H loss reaction from the parent cation, two isomeric ions can potentially be formed (*cf.* Fig. 4 and Table 1), namely H_2CNC^+ or H_2CCN^+ . According to our theoretical results, the dissociative photoionization pathway (a) $\text{CH}_3\text{NC} + h\nu \rightarrow \text{H}_2\text{CCN}^+ + \text{H} + \text{e}^-$ is energetically lower, by 0.618 eV, compared to the channel (b) $\text{CH}_3\text{NC} + h\nu \rightarrow \text{H}_2\text{CNC}^+ + \text{H} + \text{e}^-$ forming an isomeric $\text{C}_2\text{H}_2\text{N}^+$ ion. Indeed, the computed appearance energy at the PBE0/aug-cc-pVDZ(opt)//(R)CCSD(T)-F12/cc-pVTZ-F12 (+CV+SR+ZPVE) (SP) level of theory for the formation of H_2CCN^+ is $\text{AE}_{\text{calc}}(\text{H}_2\text{CCN}^+ + \text{H}) = 12.881$ eV. This value is in excellent agreement with the experimentally measured energy $\text{AE}_{\text{exp}} = 12.80 \pm 0.05$ eV. The precision interval of

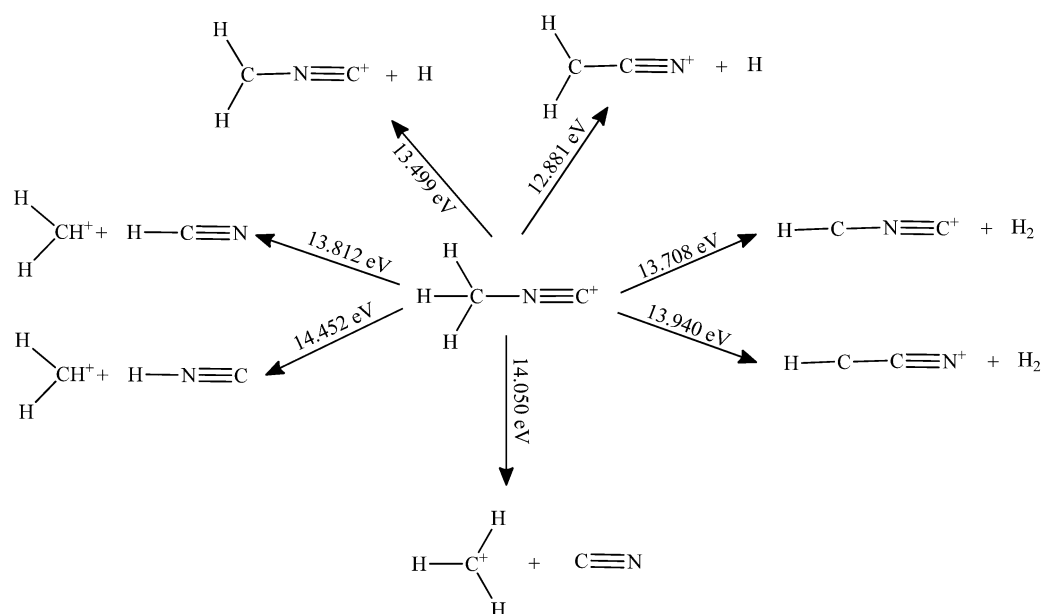


Fig. 4 Dissociative photoionization pathways and their AE calculated in this study.

the latter is only 30 meV below AE_{calc} . We can thus unambiguously assign the mass peak at m/z 40 to H_2CCN^+ , at least in the threshold region. This finding means that there is a possibility that CH_3NC isomerizes to CH_3CN before the loss of the H atom. This isomerization may occur after formation of the CH_3NC^+ ion or on the highly excited electronic states of neutral CH_3NC populated by photon absorption followed by electron ejection. At higher energies above the threshold, notably at $E > 13.5$ eV, energetically both isomeric ions could be potentially formed according to our measurements.

The experimental AE of m/z 39 (13.7 ± 0.05 eV) is in excellent agreement with the calculated AE value for the $\text{CH}_3\text{NC} + h\nu \rightarrow \text{HCNC}^+ + \text{H}_2 + e^-$ fragmentation channel (*cf.* Table 1). The calculated $AE_{\text{calc}} = 13.708$ eV is inside the precision interval of the experimental AE for this cation. The formation of the HCCN^+ isomeric form is predicted at 13.940 eV *i.e.*, about 25 meV higher than the measured AE. Thus, there would be no NC isomerization before dissociation. Hence, this fragmentation exhibits a different behavior upon absorption of photons compared to the H loss, at least at threshold. Nevertheless, the $\text{HCCN}^+ + \text{H}_2$ channel may contribute at $h\nu > 13.94$ eV.

The third observed fragmentation m/z 15 is associated with the fragmentation pathway $\text{CH}_3\text{NC} \rightarrow \text{CH}_3^+ + \text{CN}$. We measured for this fragment $AE_{\text{exp}} = 13.9 \pm 0.05$ eV, which is close to the calculated $AE_{\text{calc}} = 14.050$ eV. The difference between experimental and theoretical values is only ~ 0.1 eV.

The experimental AE of m/z 14 (13.85 ± 0.05 eV) is also in excellent agreement with the calculated AE value for the fragmentation pathway corresponding to the loss of neutral HCN (and not HNC) according to $\text{CH}_3\text{NC}^+ \rightarrow \text{CH}_2^+ + \text{HCN}$. Here, we calculated $AE_{\text{calc}} = 13.812$ eV being in excellent agreement with the experiment. Elimination of isomeric HNC, an important astrophysical molecule but less stable than HCN (by about 0.64 eV),⁶⁴ can be discarded at least in the threshold region since the corresponding fragmentation channel would be higher in energy.

3.3. Tentative assignment of the vibrational structure of the ground state TPEPICO spectrum

In order to analyze the observed vibronic structure in the TPEPICO spectrum shown in Fig. 2 we studied the neutral and cationic forms of MIC in their electronic ground states. Fig. 5 presents the calculated optimized structures of MIC and of MIC^+ as computed at the PBE0/aug-cc-pVDZ level of theory. Both species belong to the C_{3v} symmetry point group. All geometric parameters are summarized in Table 2. The molecular structures

Table 2 Main geometrical parameters (distances in Å and angles in degrees) of neutral and cationic methyl isocyanide in their electronic ground states. These data are computed at the PBE0/aug-cc-pVDZ level. See Fig. 5 for the numbering of the atoms

| Parameter | CH_3NC | CH_3NC^+ |
|-----------|------------------------|--------------------------|
| C1–H6 | 1.096 | 1.097 |
| C1–H5 | 1.096 | 1.097 |
| C1–H4 | 1.096 | 1.097 |
| C1–N2 | 1.415 | 1.431 |
| N2–C3 | 1.174 | 1.144 |
| C1–N2–C3 | 180.0 | 180.0 |
| H4–C1–H6 | 109.2 | 111.4 |
| H4–C1–H5 | 109.2 | 111.4 |
| H5–C1–H6 | 109.2 | 111.4 |

of the neutral MIC and its cation are very close. Thus, upon ionization, MIC undergoes only very minor structural modifications. For neutral MIC, our computed geometry is close to the one calculated earlier by Margulès *et al.*⁶⁵ Inspecting the geometrical parameters, we observe a small change in the bond length of the single bond C1–N2, going from 1.415 to 1.431 Å in MIC^+ and in the N2–C3 triple bond, going from 1.174 to 1.144 Å. The HCH bond angle of the methyl group changes from 109.2° to 111.4° . These small changes lead to the short vibrational progression in the TPEPICO spectrum of the ground state of MIC^+ .

We present in Table 3 the anharmonic frequencies calculations, at the PBE0/aug-cc-pVDZ level, of the eight vibrational modes of MIC^+ in its electronic ground state. These values were obtained using vibrational second-order perturbation theory. The frequencies are arranged in a descending order respectively under a_1 and e symmetry. The e symmetry normal modes ν_5^+ to ν_8^+ are doubly degenerated. In the ESI^+ we also give, in Table S5, the anharmonic frequencies of neutral MIC and compare to experimental data from the literature.⁶⁶ This table shows a reasonable agreement between our theoretical calculations and the available experimental data.

With these data, we can proceed to the assignment of the vibrationally resolved TPEPICO spectrum in the 11.1–11.8 eV photon energy range (Fig. 2). We present in Fig. 2 and Table 4 a tentative assignment of the observed progression. Guided by the geometry changes between neutral MIC and MIC^+ cation depicted above, we can fully assign these vibrational features to the pure or combination of the normal modes ν_3^+ (CH_3 symmetric deformation) and ν_4^+ (C1N2 stretching) excited upon photoionization. As noted above, the most intense transition (at $h\nu = 11.263$ eV) in the TPEPICO spectrum is assigned to the 0_0^0 origin of the progression of the transition from the neutral

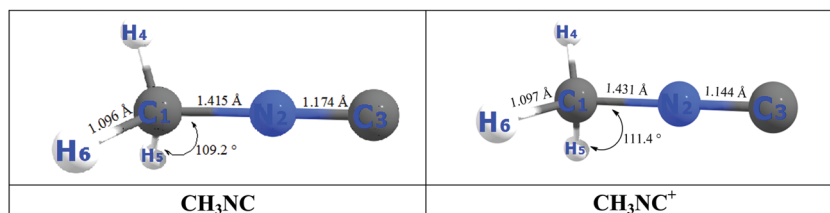


Fig. 5 Equilibrium structure of the ground state of neutral methyl isocyanide and its cation. We also give the atom numbering used in the present study.

Table 3 PBE0/aug-cc-pVDZ anharmonic frequencies (ν , cm^{-1}) of the vibrational modes of CH_3NC^+ and the type of vibration. Those of the neutral species are given in Table S5 of the ESI

| No. | Sym. | ν^+ | Type of vibration |
|---------|-------|---------|-----------------------------|
| ν_1 | a_1 | 3071 | CH_3 s-stretching |
| ν_2 | a_1 | 2426 | NC stretching |
| ν_3 | a_1 | 1404 | CH_3 s-deformation |
| ν_4 | a_1 | 888 | CN stretching |
| ν_5 | e | 3188 | CH_3 d-stretching |
| ν_6 | e | 1418 | CH_3 d-deformation |
| ν_7 | e | 1102 | CH_3 rocking |
| ν_8 | e | 324 | CNC bending |

ground state to the fundamental state of the cation. For the low intensity band peaking at 11.369 eV (855 cm^{-1} above the origin) we propose excitation of the C1N1 stretching mode ν_4^+ with one quantum. The computed value for this mode in the cation (888 cm^{-1}) confirms this assignment. We can also propose the assignment of the band at 11.437 eV (1403 cm^{-1} above the origin) to the population of the vibrational mode ν_3^+ corresponding to the excitation of the deformation vibration of the CH_3 with one quantum. This assignment has also been proposed in ref. 26 and is supported by the observation of an isotopic red shift, of $\nu_{\text{H}}/\nu_{\text{D}} = 1.33$, observed for CD_3NC in their study. The other bands can be assigned as the combination excitation of the ν_3^+ with the ν_4^+ modes. The intense band at 11.544 eV (2266 cm^{-1} above the origin) can be assigned to a combined excitation of the ν_3^+ + ν_4^+ modes, with respectively one quantum. This is in good agreement with our frequency calculations $\nu_3^+ + \nu_4^+$ calculated to be 2292 cm^{-1} . We note, however, that it has been proposed earlier (based on experiments only) that this band could be due to N2–C3 stretching excitation.²⁶ This assignment is supported by the absence of an isotopic shift in the HeI photoelectron spectrum of CD_3NC ²⁶ for this band, and in line with the change of the N2–C3 bond length found in our study. But it is in slight disagreement with our frequency calculation of the NC stretching vibration of $\nu_2^+ = 2426 \text{ cm}^{-1}$ which is off by 160 cm^{-1} from the experimental band. We therefore favor the $\nu_3^+ + \nu_4^+$ assignment for the band at 11.544 eV (*cf.* also the expected accuracy of our frequency calculations from Table S5, ESI†).

We finally propose that the band at 11.638 eV (3024.6 cm^{-1} above the origin) can be assigned to $\nu_3^+ + 2\nu_4^+$ calculated to lie at 3180 cm^{-1} . The band at 11.715 eV (3645.6 cm^{-1} above the origin)

Table 4 Tentative assignment for the experimentally observed vibrational frequencies of the photoionization bands from the ground state TPEPICO (Fig. 2)

| Band origin [eV] | Exp. frequency [cm^{-1}] | Assignment |
|------------------|-------------------------------------|-----------------------|
| 11.263 | 0.0 ^a | Adiabatic IE, 0_0^0 |
| 11.369 | 855 | ν_4^+ |
| 11.437 | 1403 | ν_3^+ |
| 11.544 | 2266 | $\nu_3^+ + \nu_4^+$ |
| 11.638 | 3025 | $\nu_3^+ + 2\nu_4^+$ |
| 11.715 | 3646 | $2\nu_3^+ + \nu_4^+$ |

^a Used as reference.

can be assigned to $2\nu_3^+ + \nu_4^+$ with a calculated frequency of 3696 cm^{-1} .

Fig. 2 presents the simulated spectrum as described in Section 2.2. An overall agreement between the measured and calculated spectra is noticeable in Fig. 2. However, one can see that some of the computed bands did not match the experimental ones *e.g.* the one assigned to $3_0^1 + 4_0^1$ combination mode. This is may be due to the non-consideration of anharmonic resonances during the computations of the FC factors. Further extensive treatments are needed as those performed recently for adenine.⁵⁷

4. Conclusion

In this work, we have presented a combined experimental and theoretical study of the photoionization and dissociative photoionization of methyl isocyanide in the gas phase, from its IE up to 15.5 eV. The experiments were done by means of VUV synchrotron radiation from the DESIRS beamline of the Synchrotron Soleil in connection with the DELICIOUS 3 spectrometer. Photoionization mass spectra, TPEPICO and PEPICO spectra were recorded. The experiments were interpreted with the help of *ab initio* quantum chemical calculations. Notably, we calculated the adiabatic ionization energy and appearance energies of fragment cations. The experimental adiabatic ionization energy is found at $\text{AIE}_{\text{exp}} = 11.263 \pm 0.005 \text{ eV}$, from the 0_0^0 band origin of the vibrational progression corresponding to the $\text{CH}_3\text{NC}(\text{X}) + h\nu \rightarrow \text{CH}_3\text{NC}^+(\text{X}) + \text{e}^-$ photoionization transition. It is in excellent agreement with a PBE0/aug-cc-pVDZ (opt)//(R)CCSD(T)-F12/cc-pVTZ-F12 (+CV+SR+ZPVE) (SP) level of theory determination ($\text{AE}_{\text{calc}} = 11.265 \text{ eV}$). From the ionization energy up to 12.8 eV the CH_3NC^+ cation is stable. Above this energy, the CH_3NC^+ intensity drops to zero and four dissociative photoionization reactions have been observed in the energy range of our study, with the H loss reaction being highest in yield. The respective appearance energies (AEs) have been measured, for m/z 40, 39, 15 and 14 cations. In order to analyze further the corresponding reactions, AE calculations have been performed at the same level of theory as the AIE calculations. As discussed in this study, the excellent agreement between measured and calculated appearance energies allowed for the assignment of the particular fragmentation pathways by dissociative photoionization of CH_3NC to form respectively $\text{H}_2\text{CCN}^+ + \text{H}$, $\text{HCNC}^+ + \text{H}_2$, $\text{CH}_3^+ + \text{CN}$, and $\text{CH}_2^+ + \text{HCN}$ with ascending photon energy. Furthermore, we calculated equilibrium geometries of the CH_3NC neutral molecule and the monocation as well as the anharmonic frequencies of both species. Thanks to these theoretical results, the vibrational progression of the cation ground state TPEPICO spectrum has been fully assigned. Finally, an important result of the present study that deserves to be further stressed is the very good performance of the PBE0/aug-cc-pVDZ (opt)//(R)CCSD(T)-F12/cc-pVTZ-F12 (+CV+SR+ZPVE) (SP) composite scheme. This approach, despite the low computational cost, is suitable for providing precise predictions for ionization and fragmentation

thresholds close to experimental accuracy, in the case of medium-sized molecules.

Conflicts of interest

There are no conflicts to declare.

Acknowledgements

This work was supported by the Programme National “Physique et Chimie du Milieu Interstellaire” (PCMI) of CNRS/INSU with INC/INP co-funded by CEA and CNES. We thank the COST ACTION CM 1401 “Our Astro-chemical history” and COST ACTION CM 1405 “Molecules in Motions” for support. We are indebted to the general technical staff of Synchrotron SOLEIL for running the facility under proposals 20141309 and 20170203. J.-C. G. thanks the Centre National d’Etudes Spatiales (CNES) for a financial support. We would like also to thank Jean-François Gil for his technical help on the SAPHIRS molecular beam chamber. We thank Lionel Poisson, Dušan Božanić and Gustavo Garcia for precious help during the measurement campaigns at SOLEIL. We acknowledge the use of the computing center MesoLUM of the LUMAT research federation (FR LUMAT 2764).

References

- 1 Cf. for example the Cologne data base for Molecular spectroscopy <https://cdms.astro.uni-koeln.de/classic/molecules>.
- 2 S. Bottinelli, C. Ceccarelli, B. Lefloch, J. P. Williams, A. Castets, E. Caux, S. Cazaux, S. Maret, B. Parise and A. G. G. M. Tielens, Complex Molecules in the hot core of the low mass protostar NGC 1333 IRAS 4A, *Astrophys. J.*, 2004, **615**, 354.
- 3 A. Belloche, H. S. P. Müller, K. M. Menten, P. Schilke and C. Comito, Complex organic molecules in the interstellar medium: IRAM 30 m line survey of Sagittarius B2(N) and (M), *Astronom. Astrophys.*, 2013, **559**, A47.
- 4 A. Belloche, R. T. Garrod, H. S. P. Müller and K. M. Menten, Detection of a branched alkyl molecule in the interstellar medium: iso-propyl cyanide, *Science*, 2014, **345**, 1584.
- 5 A. López, B. Tercero, Z. Kisiel, A. M. Daly, C. Bermúdez, H. Calcutt, N. Marcelino, S. Viti, B. J. Drouin, I. R. Medvedev, C. F. Neese, L. Pszczółkowski, J. L. Alonso and J. Cernicharo, Laboratory characterization and astrophysical detection of vibrationally excited states of vinyl cyanide in Orion-KL, *Astron. Astrophys.*, 2014, **572**, A44.
- 6 S. Zeng, D. Quénard, I. Jiménez-Serra, J. Martín-Pintado, V. M. Rivilla, L. Testi and R. Martín-Doménech, First Detection of the Prebiotic Molecule Glycolonitrile (HOCH₂CN) in the Interstellar Medium, *Mon. Not. R. Astron. Soc.*, 2019, **484**, L43–L48.
- 7 B. A. McGuire, A. M. Burkhardt, S. V. Kalenskii, C. N. Shingledecker, A. J. Remijan, E. Herbst and M. C. McCarthy, Detection of the Aromatic Molecule Benzonitrile, c-C₆H₅CN, in the Interstellar Medium, *Science*, 2018, **359**, 202–205.
- 8 P. Schilke, D. J. Benford, T. R. Hunter, D. C. Lis, T. G. Philipps and A. Line, Survey of Orion KL from 607 to 725 GHz, *Astrophys. J., Suppl. Ser.*, 2001, **132**, 281–364.
- 9 W. M. Irvine and F. P. Schloerb, Cyanide and Isocyanide abundances in the cold, dark cloud TMC-1, *Astrophys. J.*, 1984, **282**, 516–521.
- 10 J. Cernicharo, C. Kahane, M. Guélin and J. Gomez-Gonzalez, Tentative detection of CH₃NC towards Sgr B2, *Astron. Astrophys.*, 1988, **189**, L1–L2.
- 11 A. J. Remijan, J. M. Hollis, F. J. Lovas, D. F. Plusquellic and P. R. Jewell, Interstellar isomers: the importance of bonding energy differences, *Astrophys. J.*, 2005, **632**, 333–339.
- 12 P. Gratier, J. Pety, V. Guzman, J. R. Goicoechea, E. Roueff and A. Faure, The IRAM-30 m line survey of the Horsehead PDR III. High abundance of complex (iso-)nitrile molecules in UV-illuminated gas, *Astron. Astrophys.*, 2013, **557**, A101.
- 13 L. Margulès, B. Tercero, J. C. Guillemin, R. A. Motiyenko and J. Cernicharo, Submillimeter wave spectroscopy of ethyl isocyanide and its searches in Orion, *Astronom. Astrophys.*, 2018, **610**, A44.
- 14 H. Calcutt, M. R. Fiechter, E. R. Willis, H. S. P. Müller, R. T. Garrod, J. K. Jørgensen, S. F. Wampfler, T. L. Bourke, A. Coutens, M. N. Drozdovskaya, N. F. W. Ligterink and L. E. Kristensen, The ALMA-PILS survey: first detection of methyl isocyanide (CH₃NC) in a solar-type protostar, *Astronom. Astrophys.*, 2018, **617**, A95.
- 15 K. Kawaguchi, M. Ohishi and S.-I. Ishikawa, Detection of Isocyanacetylene in TMC-1, *Astrophys. J.*, 1992, **386**, L51–L53.
- 16 M. Bertin, M. Doronin, J.-H. Fillion, X. Michaut, L. Philippe, M. Lattalais, A. Markovits, F. Pauzat, Y. Ellinger and J.-C. Guillemin, Nitrile versus isonitrile adsorption at interstellar grain surfaces. I. Hydroxylated surfaces, *Astronom. Astrophys.*, 2017, **598**, A18.
- 17 M. Bertin, M. Doronin, X. Michaut, L. Philippe, A. Markovits, J.-H. Fillion, F. Pauzat, Y. Ellinger and J.-C. Guillemin, Nitrile versus isonitrile adsorption at interstellar grain surfaces. II. Carbonaceous aromatic surfaces, *Astronom. Astrophys.*, 2017, **608**, A50.
- 18 R. L. Hudson and M. H. Moore, Reactions of nitriles in ices relevant to Titan, comets, and the interstellar medium: formation of cyanate ion, ketenimines, and isonitriles, *Icarus*, 2004, **172**, 466–478.
- 19 T. L. Nguyen, J. H. Thorpe, D. H. Bross, B. Ruscic and J. F. Stanton, Reaction of Methyl Isocyanide to Acetonitrile: A High-Level Theoretical Study, *J. Phys. Chem. Lett.*, 2018, **9**, 2532–2538.
- 20 S. Leach, M. Schwell, S. Un, H. W. Jochims and H. Baumgärtel, VUV absorption spectroscopy of acetonitrile between 7 and 20 eV: A revisionist study, *Chem. Phys.*, 2008, **344**, 147–163.
- 21 M. Schwell, H. W. Jochims, H. Baumgärtel and S. Leach, VUV photophysics of acetonitrile: fragmentation, fluorescence and ionization in the 7–22 eV region, *Chem. Phys.*, 2008, **344**, 164–175.
- 22 S. Leach, G. A. Garcia, Y. Bénilan, N. Fray, M. C. Gazeau, F. Gaie-Levrel, N. Champion and M. Schwell, Ionization

- photophysics and spectroscopy of cyanoacetylene, *J. Chem. Phys.*, 2014, **140**, 184304.
- 23 N. Fray, Y. Bénilan, M. C. Gazeau, A. Jolly, M. Schwell, E. Arzoumanian, T. Ferradaz, Et. Es-Sebbar and J. C. Guillemin, Temperature dependent photoabsorption cross section of cyanodiacetylene in the vacuum UV, *J. Geophys. Res.: Planets*, 2010, **115**, E06010.
 - 24 A. Bellili, M. Schwell, Y. Bénilan, N. Fray, M. C. Gazeau, M. M. Al-Mogren, J. C. Guillemin, L. Poisson and M. Hochlaf, VUV photoionization and dissociative photoionization of the prebiotic molecule acetyl cyanide: Theory and experiment, *J. Chem. Phys.*, 2014, **141**, 134311.
 - 25 A. Bellili, M. Schwell, Y. Bénilan, N. Fray, M. C. Gazeau, M. M. Al-Mogren, J. C. Guillemin, L. Poisson and M. Hochlaf, VUV photoionization and dissociative photoionization spectroscopy of the interstellar molecule aminoacetonitrile: Theory and experiment, *J. Mol. Spectrosc.*, 2015, **315**, 196–215.
 - 26 R. F. Lake and H. W. Thompson, The photoelectron spectra of methyl isocyanide and trideuteromethyl isocyanide, *Spectrochim. Acta*, 1970, **27A**, 783–786.
 - 27 J. W. Bevan, C. Sandorfy, F. Pang and J. E. Boggs, The photoelectron spectrum of methylisocyanide-borane, *Spectrochim. Acta*, 1981, **37A**, 601–604.
 - 28 L. Asbrink, W. Von Niessen and G. Bieri, 30.4-nm He(II) photoelectron spectra of organic molecules, *J. Electron Spectrosc. Relat. Phenom.*, 1980, **21**, 93–101.
 - 29 M. N. R. Ashfold and J. P. Simons, Vacuum Ultraviolet Photodissociation Spectroscopy of CH₃CN, CD₃CN, CF₃CN and CH₃NC, *J. Chem. Soc., Faraday Trans. 2*, 1977, **74**, 1263–1274.
 - 30 T. Baer and R. P. Tuckett, Advances in threshold photoelectron spectroscopy (TPES) and threshold photoelectron photoion coincidence (TPEPICO), *Phys. Chem. Chem. Phys.*, 2017, **19**, 9698–9723.
 - 31 G. A. Garcia, B. K. Cunha de Miranda, M. Tia, S. Daly and L. Nahon, DELICIOUS III: a multipurpose double imaging particle coincidence spectrometer for gas phase vacuum ultraviolet photodynamics studies, *Rev. Sci. Instr.*, 2013, **84**, 053112.
 - 32 R. E. Schuster, J. E. Scott and A. Casanova Jr., Methyl Isocyanide, *Org. Synth.*, 1966, **46**, 75–78.
 - 33 M. J. Frisch, G. W. Trucks, H. B. Schlegel, G. E. Scuseria, M. A. Robb, J. R. Cheeseman and H. Nakatsuji, *Gaussian 09, Revision E. 01*, Gaussian, Inc., Wallingford CT, 2009.
 - 34 H.-J. Werner, P. J. Knowles, G. Knizia, F. R. Manby, M. Schütz, P. Celani, T. Korona, R. Lindh, A. Mitrushenkov and G. Rauhut, *et al.*, MOLPRO, ab initio programs package, 2015, <http://www.molpro.net>.
 - 35 C. Adamo and V. Barone, Toward Reliable Density Functional Methods Without Adjustable Parameters: The PBE0 Model, *J. Chem. Phys.*, 1999, **110**, 6158–6170.
 - 36 T. H. Dunning, Gaussian Basis Sets for Use in Correlated Molecular Calculations. I. The Atoms Boron Through Neon and Hydrogen, *J. Chem. Phys.*, 1989, **90**, 1007–1023.
 - 37 R. A. Kendall, T. H. Dunning Jr and R. J. Harrison, Electron affinities of the first-row atoms revisited. Systematic basis sets and wave functions, *J. Chem. Phys.*, 1992, **96**, 6796–6806.
 - 38 T. B. Adler, G. Knizia and H.-J. Werner, A simple and efficient CCSD(T)-F12 approximation, *J. Chem. Phys.*, 2007, **127**, 221106.
 - 39 H.-J. Werner, G. Knizia and F. R. Manby, Explicitly correlated coupled cluster methods with pair-specific geminals, *Mol. Phys.*, 2011, **109**, 407–417.
 - 40 G. Knizia, T. B. Adler and H.-J. Werner, Simplified CCSD(T) – F12 methods: theory and benchmarks, *J. Chem. Phys.*, 2009, **130**, 054104.
 - 41 K. A. Peterson, T. B. Adler and H.-J. Werner, Systematically convergent basis sets for explicitly correlated wavefunctions: the atoms H, He, B-Ne, and Al-Ar, *J. Chem. Phys.*, 2008, **128**, 084102.
 - 42 F. A. Weigend, A fully direct RI-HF algorithm: Implementation, optimised auxiliary basis sets, demonstration of accuracy and efficiency, *Phys. Chem. Chem. Phys.*, 2002, **4**, 4285–4291.
 - 43 C. Hättig, Optimization of auxiliary basis sets for RI-MP2 and RI-CC2 calculations: Core-valence and quintuple- ζ basis sets for H to Ar and QZVPP basis sets for Li to Kr, *Phys. Chem. Chem. Phys.*, 2005, **7**, 59–66.
 - 44 W. Klopper, Highly accurate coupled-cluster singlet and triplet pair energies from explicitly correlated calculations in comparison with extrapolation techniques, *Mol. Phys.*, 2001, **99**, 481–507.
 - 45 K. E. Yousaf and K. A. Peterson, Optimized auxiliary basis sets for explicitly correlated methods, *J. Chem. Phys.*, 2008, **129**, 184108.
 - 46 G. Rauhut, G. Knizia and H.-J. Werner, Accurate calculation of vibrational frequencies using explicitly correlated coupled-cluster theory, *J. Chem. Phys.*, 2009, **130**, 054105.
 - 47 K. A. Peterson, Accurate correlation consistent basis sets for molecular core-valence correlation effects: The second row atoms Al-Ar, and the first row atoms B-Ne revisited, *J. Chem. Phys.*, 2002, **117**, 10548–10560.
 - 48 M. Douglas and N. M. Kroll, Quantum electrodynamic corrections to the fine structure of helium, *Ann. Phys.*, 1974, **82**, 89–155.
 - 49 G. Jansen and B. A. Hefß, Revision of the Douglas-Kroll transformation, *Phys. Rev. A: At., Mol., Opt. Phys.*, 1989, **39**, 6016.
 - 50 W. A. De Jong, R. J. Harrison and D. A. Dixon, Parallel Douglas-Kroll energy and gradients in NWChem: estimating scalar relativistic effects using Douglas-Kroll contracted basis sets, *J. Chem. Phys.*, 2001, **114**, 48–53.
 - 51 Y. Pan, K.-C. Lau, L. Poisson, G. A. Garcia, L. Nahon and M. Hochlaf, Slow Photoelectron Spectroscopy of 3-Hydroxyisoquinoline, *J. Phys. Chem. A*, 2013, **117**, 8095–8102.
 - 52 M. Hochlaf, Advances in spectroscopy and dynamics of small and medium sized molecules and clusters, *Phys. Chem. Chem. Phys.*, 2017, **19**, 21236–21261.
 - 53 I. Derbali, H. R. Hrodmarsson, Z. Gouid, M. Schwell, M. C. Gazeau, J.-C. Guillemin, M. Hochlaf, M. E. Alikhani and E.-L. Zins, Photoionization and dissociative photoionization of propynal in the gas phase: theory and experiment, *Phys. Chem. Chem. Phys.*, 2019, **21**, 14053–14062.
 - 54 Z. Chen, K.-C. Lau, G. A. Garcia, L. Nahon, D. K. Božanic, L. Poisson, M. M. Al-Mogren, M. Schwell, J. S. Francisco,

- A. Bellili and M. Hochlaf, Identifying Cytosine-Specific Isomers via High-Accuracy Single Photon Ionization, *J. Am. Chem. Soc.*, 2016, **138**, 16596–16599.
- 55 Y. Pan, K.-C. Lau, M. M. Al-Mogren, A. Mahjoub and M. Hochlaf, Theoretical studies of 2-quinolinol: Geometries, vibrational frequencies, isomerization, tautomerism, and excited states, *Chem. Phys. Lett.*, 2014, **613**, 29–33.
- 56 Y. Majdi, M. Hochlaf, Y. Pan, K. C. Lau, L. Poisson, G. A. Garcia, L. Nahon, M. M. Al-Mogren and M. Schwell, Theoretical and Experimental Photoelectron Spectroscopy Characterization of the Ground State of Thymine Cation, *J. Phys. Chem. A*, 2015, **119**, 5951–5958.
- 57 H. Y. Zhao, K. C. Lau, G. A. Garcia, L. Nahon, S. Carniato, L. Poisson, M. Schwell, M. M. Al-Mogren and M. Hochlaf, Unveiling the complex vibronic structure of the canonical adenine cation, *Phys. Chem. Chem. Phys.*, 2018, **20**, 20756–20765.
- 58 J. Bloino, M. Biczysko, F. Santoro and V. Barone, General Approach to Compute Vibrationally Resolved One-Photon Electronic Spectra, *J. Chem. Theory Comput.*, 2010, **6**, 1256–1274.
- 59 V. Barone, J. Bloino, M. Biczysko and F. Santoro, Fully Integrated Approach to Compute Vibrationally Resolved Optical Spectra: From Small Molecules to Macrosystems, *J. Chem. Theory Comput.*, 2009, **5**, 540–554.
- 60 J. Bloino, M. Biczysko, O. Crescenzi and V. Barone, Integrated computational approach to vibrationally resolved electronic spectra: Anisole as a test case, *J. Chem. Phys.*, 2008, **128**, 244105.
- 61 J. Bloino, A. Baiardi and M. Biczysko, Aiming at an accurate prediction of vibrational and electronic spectra for medium-to-large molecules: An overview, *Int. J. Quantum Chem.*, 2016, **116**, 1543–1574.
- 62 P. W. Harland and B. J. McIntosh, Enthalpies of formation for the isomeric ions H_xCCN^+ and H_xCNC^+ ($x = 0-3$) by monochromatic electron impact on C_2N_2 , CH_3CN and CH_3NC , *Int. J. Mass Spectrom. Ion Processes*, 1985, **67**, 29–46.
- 63 W. Heerma and J. J. de Ridder, The electron-impact induced fragmentation of some alkyl isocyanides and alpha-branched alkyl cyanides, *Org. Mass Spectrom.*, 1970, **3**, 1439–1456.
- 64 T. Van Mourik, G. J. Harris, O. L. Polyansky, J. Tennyson, A. G. Császár and P. J. Knowles, Ab initio global potential, dipole, adiabatic, and relativistic correction surfaces for the HCN-HNC system, *J. Chem. Phys.*, 2001, **115**, 3706–3718.
- 65 L. Margulès, J. Demaison and H. D. Rudolph, Ab initio and experimental structures of CH_3NC , *J. Mol. Struct.*, 2001, **599**, 23–30.
- 66 T. Shimanouchi, *Tables of Molecular Vibrational Frequencies; Consolidated, NSRDS-NBS 39*, National Bureau of Standards, Washington, DC, vol. I, 1972.